AMPA receptor inhibition by synaptically released zinc

Bopanna I. Kalappa[a], Charles T. Anderson[a], Jacob M. Goldberg[b], Stephen J. Lippard[b], and Thanos Tzounopoulos[a,c,1]

[a]Department of Otolaryngology, University of Pittsburgh, Pittsburgh, PA 15261; [b]Department of Chemistry, Massachusetts Institute of Technology, Cambridge, MA 02139; and [c]Department of and Neurobiology, University of Pittsburgh, Pittsburgh, PA 15261

Edited by Robert C. Malenka, Stanford University School of Medicine, Stanford, CA, and approved November 9, 2015 (received for review June 23, 2015)

The vast amount of fast excitatory neurotransmission in the mammalian central nervous system is mediated by AMPA-subtype glutamate receptors (AMPARs). As a result, AMPAR-mediated synaptic transmission is implicated in nearly all aspects of brain development, function, and plasticity. Despite the central role of AMPARs in neurobiology, the fine-tuning of synaptic AMPA responses by endogenous modulators remains poorly understood. Here we provide evidence that endogenous zinc, released by single presynaptic action potentials, inhibits synaptic AMPA currents in the dorsal cochlear nucleus (DCN) and hippocampus. Exposure to loud sound reduces presynaptic zinc levels in the DCN and abolishes zinc inhibition, implicating zinc in experience-dependent AMPAR synaptic plasticity. Our results establish zinc as an activity-dependent, endogenous modulator of AMPARs that tunes fast excitatory neurotransmission and plasticity in glutamatergic synapses.

AMPA receptors | zinc | ZnT3 | synaptic plasticity | auditory

The development, function, and experience-dependent plasticity of the mammalian brain depend on the refined neuronal interactions that occur in synapses. In the majority of excitatory synapses, the release of the neurotransmitter glutamate from presynaptic neurons opens transmembrane ion channels in postsynaptic neurons, the ionotropic glutamate receptors, thereby generating the flow of excitatory signaling in the brain. As a result, these receptors play a fundamental role in normal function and development of the brain, and they are also involved in many brain disorders (1).

The ionotropic glutamate receptor family consists of AMPA, kainate, and NMDA receptors (NMDARs). Although kainate receptor-mediated excitatory postsynaptic responses occur in a few central synapses (2), AMPA receptors (AMPARs) and NMDARs are localized in the postsynaptic density of the vast majority of glutamatergic synapses in the brain, mediating most of excitatory neurotransmission (1). NMDAR function is regulated by a wide spectrum of endogenous allosteric neuromodulators that fine-tune synaptic responses (3–5); however, much less is known about endogenous AMPAR neuromodulators [(1, 5), but see refs. 6 and 7]. Recent structural studies revealed that the amino terminal domain (ATD) and ligand-binding domain (LBD) are tightly packed in NMDARs but not AMPARs (8–10). These structural differences explain some of the functional differences in allosteric modulation between AMPARs and NMDARs, such as why the ATD of NMDARs, unlike that of AMPARs, modulates function and contains numerous binding sites for allosteric regulators. Nonetheless, given the importance of fine-tuning both synaptic AMPAR and NMDAR responses for brain function, it is puzzling that there is not much evidence for endogenous, extracellular AMPAR modulation. The discovery and establishment of endogenous AMPAR modulators is crucial both for understanding ionotropic glutamate receptor signaling and for developing therapeutic agents for the treatment of AMPAR-related disorders, such as depression, cognitive dysfunctions associated with Alzheimer's disease, and schizophrenia (1, 11).

Free, or readily chelatable, zinc is an endogenous modulator of synaptic and extrasynaptic NMDARs (12–15). Free zinc is stored in glutamatergic vesicles in many excitatory synapses in the cerebral cortex, limbic, and brainstem nuclei (16). In some brain areas, such as in the hippocampus, 50% of boutons synapsing onto CA1 neurons and all mossy fibers synapsing onto CA3 neurons contain synaptic free zinc (17). Whereas earlier studies demonstrated that exogenous zinc inhibits AMPARs (18–21), more recent work suggests that endogenously released synaptic zinc does not modulate AMPARs in central synapses (14, 22). This conclusion was derived from the inability to efficiently chelate and quantify synaptic zinc with the zinc-selective chelators and probes used (15), in apparent support of the hypothesized low levels of released zinc during synaptic stimulation (14).

Recent work in our laboratories used new chemical tools that allowed us to intercept and visualize mobile zinc efficiently (15). These studies revealed modulation of extrasynaptic NMDARs by zinc and led us to reinvestigate whether synaptically released zinc might be an endogenous modulator of AMPARs as well. In the present study, we applied these same tools in electrophysiological, laser-based glutamate uncaging and in imaging experiments using wild type and genetically modified mice that lack synaptic zinc.

Results

ZnT3-Dependent Synaptic Zinc Inhibits AMPAR EPSCs in Dorsal Cochlear Nucleus Synapses. First, we explored the effect of synaptic zinc on AMPAR-mediated excitatory postsynaptic currents (EPSCs) in the dorsal cochlear nucleus (DCN), a zinc-rich auditory brainstem nucleus. The DCN is a cerebellum-like structure (23), where glutamatergic parallel fibers (PFs) are zinc-rich (24) and innervate interneurons and principal neurons, cartwheel cells (CWCs), and fusiform cells (FCs), respectively. Bath application of 100 μM ZX1, an extracellular fast, high-affinity zinc chelator (13, 15), potentiated cartwheel cell AMPAR EPSCs evoked by a single PF stimulus (PF EPSCs) (Fig. 1 *A*–*C*). This finding suggested, for the first time to our knowledge in a mammalian synapse, that endogenous zinc inhibits AMPAR EPSCs.

To determine whether the effects of synaptic zinc on PF EPSCs were mediated by presynaptic mechanisms, we used paired-pulse ratio (PPR) and coefficient of variation (CV) analysis, two

Significance

Ionotropic glutamate AMPA receptors (AMPARs) play a fundamental role in normal function and plasticity of the brain, and they are also involved in many brain disorders. Despite the central role of AMPARs in neurobiology, the modulation of synaptic AMPA responses by endogenous modulators remains not well understood. Here, in three synapses found in two different brain areas, we provide the first evidence, to our knowledge, that endogenous zinc is coreleased with glutamate and modulates the strength of synaptic AMPAR responses. Because in many neocortical areas more than 50% of excitatory presynaptic terminals contain zinc within their glutamatergic vesicles, our findings establish zinc as a general neuromodulator that allows for fine-tuning and plasticity of glutamatergic fast synaptic transmission in the brain.

Author contributions: B.I.K., S.J.L., and T.T. designed research; B.I.K. and C.T.A. performed research; J.M.G. and S.J.L. contributed new reagents/analytic tools; B.I.K., C.T.A., J.M.G., and T.T. analyzed data; and B.I.K., S.J.L., and T.T. wrote the paper.

The authors declare no conflict of interest.

This article is a PNAS Direct Submission.

[1]To whom correspondence should be addressed. Email: thanos@pitt.edu.

This article contains supporting information online at www.pnas.org/lookup/suppl/doi:10.1073/pnas.1512296112/-/DCSupplemental.

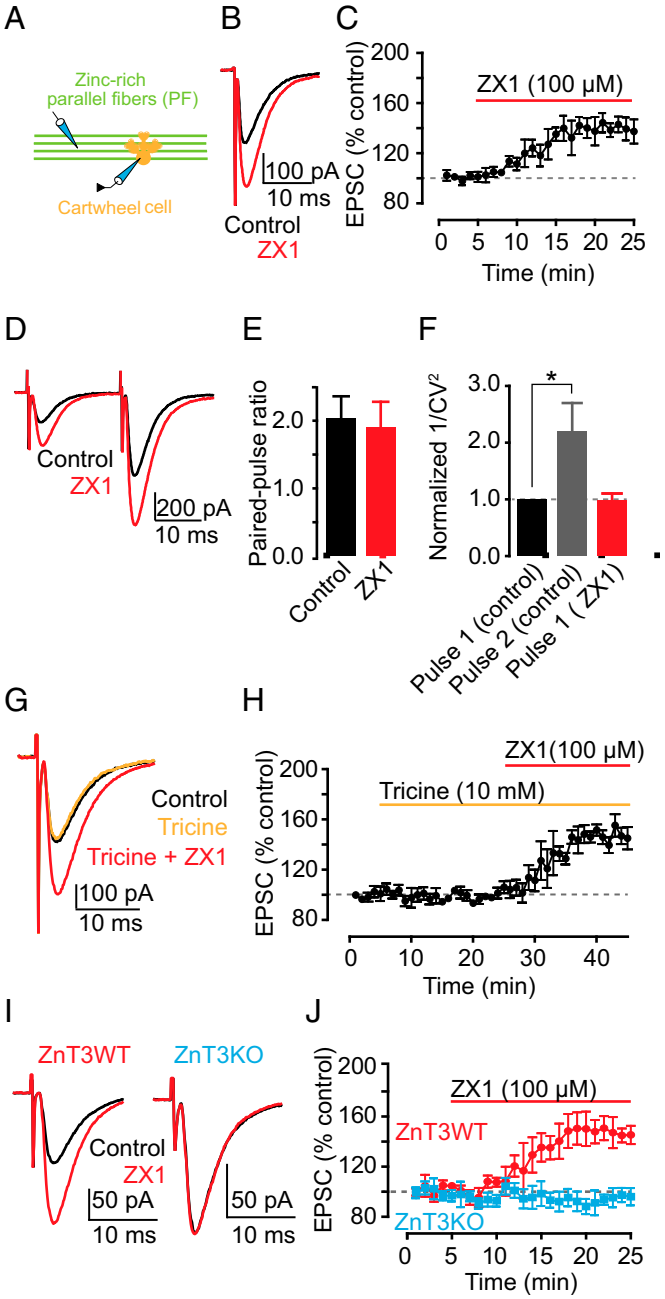

Fig. 1. Synaptic ZnT3-dependent zinc inhibits AMPAR EPSCs in DCN parallel fiber synapses via a postsynaptic mechanism. (*A*) Schematic of the experimental setup for electrophysiological experiments in cartwheel cells. In this figure, AMPAR EPSCs were recorded from cartwheel cells and evoked by parallel fiber stimulation (PF EPSCs). (*B*) Representative PF EPSCs before and after ZX1 application. (*C*) Time course of PF EPSC amplitude before and after ZX1 application (PF EPSC amplitude, 15–20 min after ZX1 application: 140.22 ± 7.66% of baseline, $n = 7$, $P < 0.01$). (*D*) Representative PF EPSCs in response to two stimuli 20 ms apart: before and after ZX1 application. (*E*) Summary graph of paired-pulse ratio ($n = 7$, $P = 0.36$ for control vs. ZX1). (*F*) Summary graph of normalized $1/CV^2$ ($n = 7$, $P = 0.01$ for second pulse vs. first pulse; $n = 7$, $P = 0.95$ for control first pulse vs. ZX1 first pulse). (*G*) Representative PF EPSCs in control, after tricine, and after tricine and ZX1 application. (*H*) Time course of PF AMPAR EPSC amplitude before, after tricine, and after tricine and ZX1 application (PF EPSC amplitude: 15–20 min after tricine application: 100.07 ± 3.35% of baseline, $n = 5$, $P = 0.97$; 15–20 min after tricine and ZX1 application: 146.51 ± 7.20% of baseline, $n = 5$, $P < 0.01$). (*I*) Representative PF EPSCs from ZnT3WT and ZnT3KO mice before and after ZX1 application. (*J*) Time course of PF EPSC amplitude from ZnT3WT and ZnT3KO mice before and after ZX1 application (PF EPSC amplitude, 15–20 min after ZX1 application: ZnT3WT: 147.02 ± 8.82% of baseline, $n = 5$, $P < 0.01$; ZnT3KO: 94.69 ± 6.85% of baseline, $n = 5$, $P = 0.16$; ZnT3WT vs. ZnT3KO: $P < 0.01$). Values represent mean ± SEM. For details of statistical tests and detailed values shown in main figures, see *SI Materials and Methods*.

assays that are sensitive to changes in presynaptic probability of neurotransmitter release [Pr (25, 26)]. PPR, the ratio of the amplitude of the second EPSC to the first EPSC evoked by two stimuli applied in rapid succession (Fig. 1*D*), depends on Pr. High Pr synapses show paired-pulse depression, whereas low Pr synapses show paired-pulse facilitation. CV, which is the standard deviation (SD) of the EPSC amplitudes normalized to the mean amplitude, varies inversely with quantal content. The inverse square, $1/CV^2$, is directly proportional to quantal content, where quantal content = n Pr, n being the number of release sites. ZX1 did not alter either PPR or $1/CV^2$ of PF EPSCs, indicating a lack of contribution of presynaptic mechanisms in the zinc-mediated depression in PF EPSCs (Fig. 1 *E* and *F*). As expected, $1/CV^2$ of the second pulse in control conditions was increased, consistent with increased Pr of the second stimulus (Fig. 1*F*). Previous studies showed that endogenous zinc inhibits Pr via endocannabinoid signaling in DCN synapses (22). However, this effect required prolonged high frequency presynaptic stimulation. To further interrogate the lack of presynaptic effects of zinc on PF EPSCs, we examined the influence of ZX1 in the presence of 1 μM AM-251, a cannabinoid receptor (CB1R) antagonist, which blocks endocannabinoid signaling. ZX1 enhanced PF EPSCs in the presence of AM-251 to an extent similar to that as in the absence of AM-251 (Fig. S1 *A* and *B*). Taken together, these results are consistent with the notion that endogenous zinc inhibits AMPAR EPSCs evoked by a single PF stimulus via a postsynaptic mechanism.

At hippocampal mossy-fiber (MF) to CA3 zinc-rich synapses, the use of either tricine or CaEDTA, two of the most widely used extracellular zinc chelators, did not reveal any effects on either AMPAR or NMDAR EPSCs (13, 14). CaEDTA is a slow chelator and is therefore not expected to intercept fast synaptic zinc transients (12, 13, 15). Studies using tricine, a commonly used chelator for studying the role of synaptic zinc (27), did not reveal any effect of synaptic zinc on AMPAR EPSCs, either in MF synapses onto CA3 neurons or in PF synapses onto DCN fusiform cells (14, 22). Here, by using ZX1, an extracellular zinc chelator with a second-order rate constant for binding zinc that is 200-fold higher than those for tricine and CaEDTA (15), we used the most efficient chelator for studying the effect of synaptic zinc on AMPAR neurotransmission. Indeed, bath application of 10 mM tricine did not affect PF EPSCs in CWCs (Fig. 1 *G* and *H*). However, subsequent addition of 100 μM ZX1 potentiated PF EPSCs, without affecting either PPR or CV (Fig. 1 *G* and *H* and Fig. S1 *C* and *D*). Together, these results indicate that ZX1, unlike tricine, can unmask the inhibitory effect of synaptically released zinc on baseline AMPAR synaptic transmission.

Because zinc transporter 3 (ZnT3) is the protein that loads zinc in presynaptic glutamatergic vesicles, we hypothesized that mice lacking this transporter (ZnT3KO mice), and thereby synaptic zinc (28), would not exhibit zinc-mediated modulation of AMPAR EPSCs. Consistent with this hypothesis, ZX1 potentiated PF EPSCs in ZnT3 WT mice (ZnT3WT) without affecting either PPR or CV, but did not affect PF EPSCs in ZnT3KO mice (Fig. 1 *I* and *J* and Fig. S2 *A* and *B*). PF quantal release properties (22), PPR, CV, and kinetics of postsynaptic AMPAR responses were not different between ZnT3WT and ZnT3KO mice, indicating that ZnT3KO mice have similar presynaptic properties and postsynaptic AMPARs (Fig. S2 *A*–*C* and Table S1). The lack of effect of ZX1 on PF EPSCS in ZnT3KO mice is therefore not a consequence either of changes in basal synaptic properties or changes in AMPAR composition between WT and KO mice. Moreover, these results show that the effects of ZX1 on PF EPSCs in WT mice are not due to nonspecific effects of ZX1 on synaptic AMPARs. We conclude that synaptic release

of ZnT3-dependent vesicular zinc mediates the inhibition of PF EPSCs.

Evoked Action Potential Driven Release of Zinc from Presynaptic Terminals Mediates AMPAR EPSC Inhibition. ZX1 potentiation of PF EPSCs is consistent with the hypothesis that chelation of stimulus-driven, synaptically released zinc removes AMPAR inhibition by the metal ion. Alternatively, there might be a tonic level of ZnT3-dependent zinc, arising from spontaneous release of zinc from presynaptic vesicles, which inhibits AMPARs but is independent of synaptic stimulation. Low nanomolar tonic zinc levels in DCN brain slices inhibit extrasynaptic NMDARs and potentiate glycine receptors (15, 29). To determine whether tonic zinc modulates AMPAR currents, we used glutamate uncaging to activate AMPARs and bypass synaptic stimulation. When we uncaged glutamate onto the dendritic arbor of CWCs in the molecular layer (Fig. 2*A*), we evoked pharmacologically isolated AMPAR currents that were not potentiated by the addition of ZX1. This finding indicates that tonic zinc does not modulate AMPARs and is consistent with the nanomolar zinc affinity of NMDARs containing NR2A subunits (30) and glycine receptors containing the α1 subunit (31), compared with the lower zinc affinity of AMPARs (18, 19). Moreover, ZX1 application did not affect the amplitude, frequency, or kinetics of spontaneous EPSCs (sEPSCs; Fig. 2 *D–I*), which are elicited by random, nonevoked firing of presynaptic granule cells, indicating that inhibition of PF EPSCs by zinc requires evoked, action potential-driven release of zinc from presynaptic vesicles.

Zinc Inhibition of AMPAR EPSCs Is Input Specific in DCN Synapses. The DCN is a laminar structure with layers that contain glutamatergic PF zinc-rich terminals synapsing onto different neurons, as well as layers that harbor zinc-lacking glutamatergic terminals. In particular, fusiform cells receive zinc-rich PF input at their apical dendrites in the molecular layer, and zinc-lacking auditory nerve (AN) input at their basal dendrites in the deep layer (Fig. 3*E*) (32). Moreover, fusiform cells express AMPARs containing GluA2-3 subunits in their apical dendrites, whereas cartwheel cells express GluA1-3 subunits (33). To determine whether zinc modulation of PF EPSCs is input-specific in fusiform cells and whether zinc modulates PF EPSCs in another synapse with different AMPAR composition, we took advantage of this anatomical and functional segregation of synaptic inputs in the DCN. First, we demonstrated that the DCN molecular layer is zinc-rich by using a cell-permeable, acetylated zinc fluorescent sensor diacetylated Zinpyr-1 (DA-ZP1) (34). Consistent with previous anatomical studies (32), our imaging experiments revealed a zinc-specific fluorescent signal that is ZnT3 dependent and specific to the molecular layer of the DCN (Fig. 3*A*). Next, we used an extracellular fluorescent sensor, ZP1-6COOH, to determine whether we could observe input-specific zinc release. We performed two-pathway imaging experiments in the same slice, which showed that PF stimulation in the molecular layer generated a fluorescent response, indicating zinc release, whereas stimulation of AN fibers in the deep layer did not generate any zinc fluorescence signal (Fig. 3 *B–D*). To test for input-specific inhibition of PF EPSCs by zinc, we used two-pathway electrophysiological experiments to record PF EPSCs and AN EPSCs from the same fusiform cell (Fig. 3 *E* and *F*). Note that PF EPSCs, but not AN EPSCs, showed paired-pulse facilitation, further confirming our ability to stimulate two independent, anatomically and functionally distinct inputs (Fig. 3*F* and Fig. S3*A*). Application of ZX1 potentiated only PF EPSCs without affecting PPR, but left AN EPSCs unaffected (Fig. 3 *G* and *H* and Fig. S3*A*). These results show that zinc-mediated modulation of AMPAR EPSCs in fusiform cells is input-specific, occurring only at glutamatergic synapses that contain zinc, and is mediated by postsynaptic mechanisms. Moreover, these results indicate that zinc modulates synapses with AMPARs containing GluA1-3 subunits.

Zinc Inhibition of AMPAR EPSCs in Hippocampal Synapses. To determine whether synaptic zinc-mediated inhibition of AMPAR

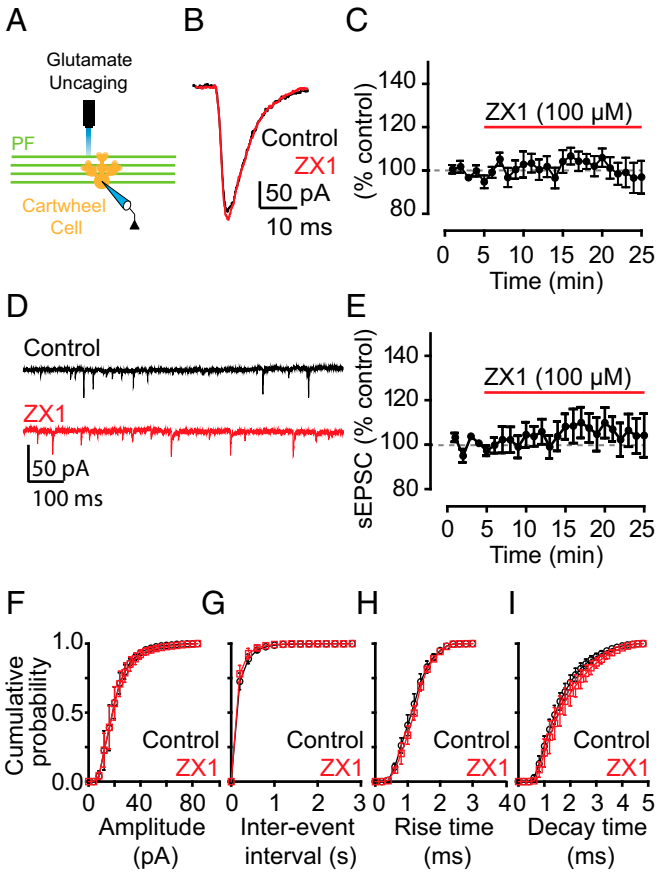

Fig. 2. Inhibition of AMPAR EPSCs by synaptic zinc is dependent on evoked, action potential-driven release of zinc from presynaptic terminals. (*A*) Schematic of the location of glutamate uncaging. (*B*) Representative AMPAR currents in response to glutamate uncaging before and after ZX1 application. (*C*) Time course of amplitude of AMPAR uncaging currents before and after ZX1 application (AMPAR current amplitude, 15–20 min after ZX1 application: 98.46 ± 6.27% of baseline, $n = 5$, $P = 0.84$). (*D*) Representative traces of spontaneous AMPAR EPSCs (sEPSCs) before and ZX1 application. (*E*) Time course of the mean sEPSC amplitude before and after ZX1 application (mean sEPSC amplitude, 15–20 min after ZX1 application: 104.34 ± 8.78% of baseline, $n = 5$, $P = 0.56$). (*F–I*) Cumulative probability plot of sEPSC amplitude (*F*), frequency (*G*), rise time (*H*), and decay time (*I*) before and after ZX1 application (mean sEPSC amplitude: $n = 5$, $P = 0.24$ for control vs. ZX1; mean sEPSC frequency: $n = 5$, $P = 0.72$ for control vs. ZX1; mean sEPSC rise time: $n = 5$, $P = 0.25$ for control vs. ZX1; mean sEPSC decay time: $n = 5$, $P = 0.10$ for control vs. ZX1).

EPSCs is a general modulatory mechanism of AMPAR neurotransmission across different zinc-containing synapses, we explored the effect of zinc on AMPAR EPSCs in the hippocampus. We stimulated zinc-rich Schaffer collateral fibers (SCs) (14) (Fig. 3*I*), and we recorded from hippocampal CA1 neurons, which express AMPARs containing GluA1-3 subunits (35). ZX1 potentiated CA1 SC EPSCs in ZnT3WT mice, but left CA1 SC EPSCs unaffected in ZnT3KO mice (Fig. 3 *J* and *K*). Similar to the DCN, ZX1 did not affect PPR and CV of SC EPSCs in ZnT3WT mice (Fig. S3 *B* and *C*), indicating that synaptic zinc modulates CA1 SC EPSCs via postsynaptic mechanisms. Finally, PPR, CV, and kinetic properties of CA1 SC EPSCs were not different between ZnT3WT and ZnT3KO mice, suggesting that the lack of effect of ZX1 in SC EPSCs in ZnT3KO mice was due to the lack of synaptic zinc and not to differences in baseline synaptic transmission between ZnT3WT and ZnT3KO mice (Fig. S3 *B–D* and Table S1). Moreover, we investigated the effects of ZX1 on the presynaptic fiber volley and the size of the accompanied field EPSP (fEPSP) recorded in the stratum radiatum and evoked

NEUROSCIENCE

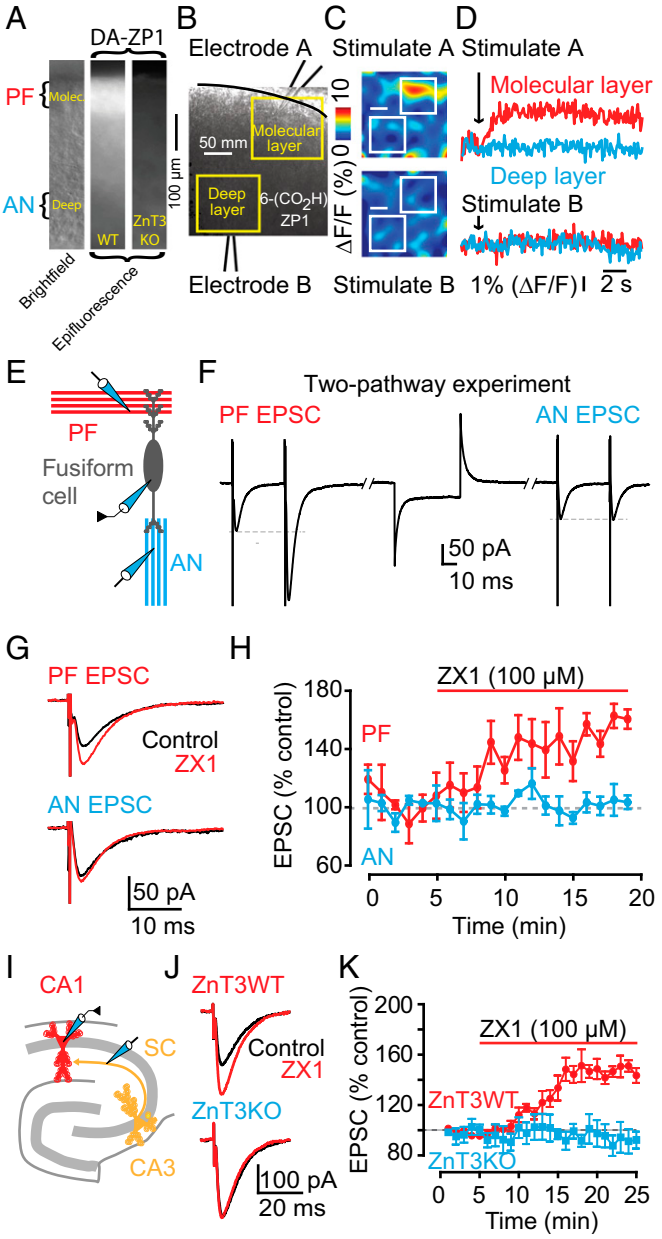

Fig. 3. Zinc-mediated inhibition of AMPAR EPSCs is input specific in DCN synapses and occurs in hippocampal synapses. (*A*, *Left*) Brightfield image of a DCN slice showing the molecular and deep layer of the DCN where parallel fiber (PF) and auditory nerve (AN) inputs reside, respectively. (*Center*) DA-ZP1, a cell-permeable fluorescent zinc sensor reveals zinc-mediated fluorescence in the molecular but not deep layer of a DCN slice from a WT mouse. (*Right*) Absence of DA-ZP1 fluorescence in a DCN slice from a ZnT3KO mouse. (*B*) Illustration of two-pathway imaging experiments with stimulating electrodes placed in the molecular and deep layer of the DCN. (*C*) In response to a 100-Hz, 1-s stimulation in the molecular layer, ZP1-6COOH, a membrane-impermeable fluorescent zinc sensor reveals evoked zinc signals in the molecular but not in the deep layer of the DCN. No fluorescence is evoked by identical electrical stimulation in the deep layer. (*D*) Representative ZP1-6COOH fluorescent responses in response to a 100-Hz, 1-s electrical stimulation. (*E*) Schematic of the experimental setup for two-pathway electrophysiological experiments in fusiform cells. (*F*) Representative traces from two-pathway experiment showing, in response to paired-pulse stimulation, PF EPSCs, and AN EPSCs recorded from the same fusiform cell. (*G*) Representative PF and AN EPSCs, recorded from the same fusiform cell as shown in *F*, before and after ZX1 application. (*H*) Time course of PF and AN EPSC amplitude before and after ZX1 application (AMPAR EPSC amplitude, 10–15 min after ZX1 application: PF EPSC: 151.09 ± 7.05% of baseline, $n = 3$, $P < 0.01$; AN EPSC: 100.01 ± 1.66% of baseline, $n = 3$, $P = 0.79$; PF EPSC vs. AN EPSC: $P < 0.01$). (*I*) Schematic of the experimental setup for experiments in the hippocampus, including stimulation of Schaffer collaterals (SC) and recording from CA1 neurons (*J*) Representative SC CA1 EPSCs from ZnT3WT and ZnT3KO mice before and after ZX1 application. (*K*) Time course of ZnT3WT and ZnT3KO SC CA1 EPSC amplitude before and after ZX1 application (AMPAR EPSC amplitude, 15–20 min after ZX1 application: ZnT3WT: 146.71 ± 5.66% of baseline; $n = 5$, $P < 0.01$; ZnT3nKO: 92.23 ± 9.20% of baseline; $n = 5$, $P = 0.18$; ZnT3WT vs. ZnT3KO: $P < 0.01$).

by afferent stimulation also in the stratum radiatum. ZX1 increased synaptic strength, measured as increases in the slope of the fEPSP, without affecting the amplitude of presynaptic fiber volley (Fig. S3 *E* and *F*). Because the amplitude of the fiber volley is proportional to the number of presynaptic fibers activated by the stimulus and thus serves as an estimate of the strength of an afferent input, we conclude that ZX1 increases synaptic strength but does not affect afferent input (Fig. S3 *E* and *F*). Next, we measured the effect of ZX1 on the spiking output of DCN granule cells, the cells from which zinc-rich parallel fibers originate. ZX1 did not affect either action potential threshold or the current-firing frequency (*f–I*) function in these neurons (Fig. S3 *G* and *H*), further suggesting that ZX1 does not affect the spiking output of presynaptic neurons. Taken together, our results suggest that zinc inhibition of AMPAR EPSCs is a general postsynaptic modulatory mechanism in zinc-containing synapses that express GluA1-3.

Plasticity of AMPAR EPSCs by Sound-Evoked Reduction of Presynaptic Zinc Levels in DCN Synapses. The results depicted in Figs. 1–3 show that synaptic zinc is an endogenous neuromodulator that controls the strength of baseline synaptic responses in zinc-containing synapses. Potential plasticity of zinc levels would give zinc a dynamic role in shaping excitatory synaptic transmission in an activity-dependent manner and would add to the complexity of synaptic plasticity in mammalian synapses. In the neocortex, levels of synaptic zinc are rapidly and dynamically regulated. In particular, in the barrel cortex, increased sensory stimulation leads to decreased levels of synaptic zinc, whereas decreased sensory stimulation leads to increased synaptic zinc (36). These anatomical studies have established the experience-dependent modulation of synaptic zinc levels; however, the effect of this modulation on synaptic strength remains unknown. We examined the effect of auditory experience on zinc-mediated effects on PF EPSCs in fusiform cells, which receive direct AN input in their basal dendrites (Fig. 3*E*). We examined mice that were exposed to sustained loud sound (see *SI Materials and Methods* for details), which caused hearing loss, as evidenced by increased threshold of auditory brainstem responses (ABRs) in noise-exposed mice (Fig. S4 *A–D*). We also studied sham-exposed mice, which underwent the same procedure but were not exposed to sound. As expected, ZX1 enhanced PF EPSCs in fusiform neurons from sham-exposed mice, but, strikingly, did not affect PF EPSCs in fusiform neurons from noise-exposed mice (Fig. 4 *A* and *B*). Moreover, PPR, CV, and kinetic properties of PF EPSCs were not different between sham- and noise-exposed mice, suggesting that the lack of an effect of ZX1 on PF EPSCs in noise-exposed mice was not a result of changes in glutamatergic synaptic transmission (Fig. S4 *E* and *F* and Table S1). Quantal analysis on stimulus-evoked AN EPSCs from sham- and noise-exposed mice showed that CV was increased in noise-exposed mice but PPR was unaltered (Fig. S4 *G* and *H*). These results indicate decreased quantal content (n Pr) without changes in Pr in sound-exposed mice; such changes are consistent with a reduced number of release sites. Moreover, these results are consistent with reduced ABR thresholds (Fig. S4 *A–D*) and with previous studies showing damage of AN terminals even after milder acoustic trauma (37, 38).

We hypothesized that the lack of a ZX1 effect on PF EPSCs may be due to a decrease in zinc inhibition in PF EPSCs. Consistent with this hypothesis, we found that DCN slices from noise-exposed mice showed a significant decrease in synaptic zinc levels,

as evidenced by reduced DA-ZP1 fluorescence in these mice (Fig. 4 *C* and *D*). Next, we compared evoked zinc release between sham- and noise-exposed mice. To quantify evoked zinc levels in DCN slices, we incubated the slices in ACSF containing the ratiometric zinc sensor LZ9 (2 μM), measured zinc-mediated fluorescence in response to PF electrical stimulation (Fig. 4*E*), and used the equation shown in *SI Materials and Methods* to convert fluorescent ratios to extracellular zinc levels, which were subsequently normalized to sham-exposed levels (15). We found that evoked zinc release was significantly reduced in noise-exposed mice (Fig. 4 *E* and *F*). This result suggests that sound-dependent reduction in vesicular zinc levels and vesicular zinc release abolished the inhibitory effect of zinc on PF AMPAR EPSCs. Because noise exposure caused reduction of AN inputs, we suggest that the sound-dependent removal of the inhibitory effect of zinc enhances PF EPSCs and is consistent with a compensatory, presynaptic homeostatic response that restores the overall excitatory strength in fusiform cells. This finding indicates that experience-dependent changes of presynaptic zinc levels caused AMPAR plasticity even in the absence of changes in glutamatergic transmission.

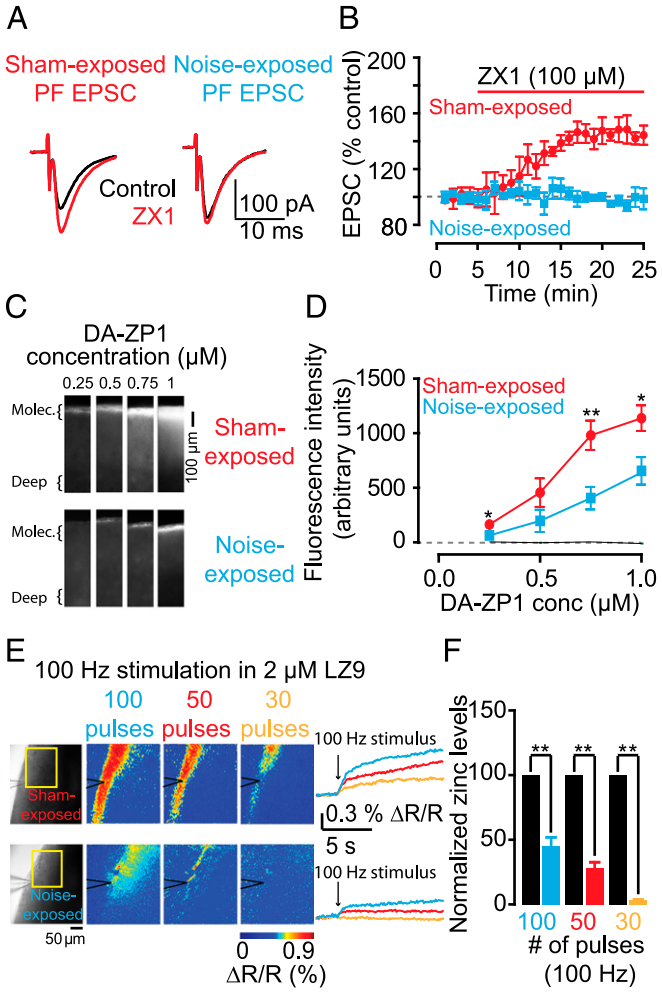

Fig. 4. Plasticity of AMPAR EPSCs by sound-evoked reduction of presynaptic zinc levels in DCN parallel fiber synapses. (*A*) Representative PF EPSCs from sham- and noise-exposed mice before and after ZX1 application. (*B*) Time course of PF EPSC amplitude from sham- and noise-exposed mice before and after ZX1 application (PF EPSC amplitude: sham-exposed: 145.55 ± 6.87% of baseline, $n = 5$, $P < 0.01$; noise-exposed: 96.98 ± 4.85% of baseline, $n = 5$, $P = 0.83$; sham- vs. noise-exposed: $P < 0.01$). (*C*) Representative zinc-mediated fluorescent signals in sham- and noise-exposed mice at increasing concentrations of DA-ZP1. (*D*) Summary graph of fluorescence intensity at different concentrations of DA-ZP1 (fluorescence intensity in arbitrary units: sham- vs. noise-exposed, $n = 5$, $P = 0.02$ for 0.25 μM; $P = 0.15$ for 0.5 μM; $P < 0.01$ for 0.75 μM; $P = 0.03$ for 1 μM). (*E*, *Left*) Representative evoked, zinc-mediated fluorescent signals in sham- and noise-exposed mice in response to increasing number of pulses at 100 Hz. (*Right*) Time course of representative ratiometric fluorescent signals. (*F*) Summary graph of normalized extracellular zinc concentrations. Concentrations from noise-exposed mice are normalized to sham-exposed average concentrations.

Discussion

Our results show that endogenous, synaptically released zinc modulates AMPAR EPSCs in two different brain areas. Although earlier studies had suggested that exogenous zinc modulates AMPARs, this modulation has been considered physiologically irrelevant, because recent work failed to reveal any effect of endogenous zinc on AMPAR EPSCs in hippocampal and in DCN synapses (14, 22). However, these studies either used tricine or compared AMPAR EPSCs between WT and ZnT3KO mice. The use of tricine is problematic, because, unlike ZX1, tricine cannot efficiently prevent zinc from binding high-affinity zinc-binding sites and therefore is not an appropriate chelator for studying the role of zinc in synapses (15). Consistent with these results, ZX1, but not tricine, revealed the effect of endogenous zinc on AMPAR EPSCs (Fig. 1 *G* and *H*).

Finally, the lack of difference in the size of AMPAR EPSCs, evoked by trains of synaptic stimuli, between WT and ZnT3KO in hippocampal synapses has been used as evidence for the lack of effect of endogenous zinc on MF AMPA EPSCs (14). However, this result does not exclude compensatory, non–zinc-mediated mechanisms that maintain AMPAR EPSCs unchanged in ZnT3KO mice. Together, our results establish vesicular zinc as an endogenous AMPAR modulator that adjusts fast excitatory synaptic transmission in the brain.

Single shocks of PFs revealed a robust ZX1 effect on PF EPSCs (Figs. 1, 3, and 4), but ZX1 application did not enhance sEPSCs (Fig. 2 *D* and *E*). These results suggest that zinc is "pooling" between release sites so as to require multisite activity to exert its inhibitory effect on AMPARs (i.e., evoked, multisynapse release). Moreover, our experiments in PF EPSCs showed no changes in the quantal content of PF glutamatergic neurotransmission after noise exposure (Fig. S4 *E* and *F*). However, our results revealed decreases in zinc content and zinc release in the same PF terminals from noise-exposed mice (Fig. 4 *C*–*F*), suggesting that activity-dependent changes in zinc-containing vesicles mediate the observed sound-dependent plasticity in presynaptic zinc levels and release (Fig. 4). These results suggest that zinc-containing vesicles may form a functionally and/or anatomically distinct population. This hypothesis is consistent with previous studies showing that ZnT3 interacts with the adaptor protein AP3 and is preferentially targeted to a distinct vesicle subpopulation (39, 40). The anatomical and functional properties of different zinc-containing synapses and the relative distribution and release dynamics of zinc-containing vesicles may determine the requirement for differential activity patterns capable of eliciting zinc modulation of AMPAR EPSCs in zinc-containing glutamatergic synapses. These differential requirements may explain the lack of effect of ZX1 in mossy fiber field potentials (13).

Whereas previous results have shown that AMPARs lacking GluA2 subunits are permeable to zinc (41), our results establish that endogenous zinc inhibits AMPAR EPSCS in zinc-containing synapses that express GluA1-3. Our results are consistent with direct binding and modulation of AMPARs by synaptic zinc. This conclusion is also consistent with structural data showing that the LBD of GluA2 contains a number of zinc binding sites formed mainly by histidine residues (42). Because the ATD and LBD are tightly packed in NMDARs but more separated in AMPARs, with the consequence that the ATD is not a regulatory site for AMPARs (8, 9), we propose that the LBD is a more likely site for allosteric AMPAR modulation by zinc. More studies are needed for determining the subunit sensitivity, the binding site, and the underlying biophysical mechanism of zinc-mediated AMPAR inhibition.

How could stimulation by noise exposure, which targets AN inputs, lead to changes in vesicular zinc in PF inputs? Recent results have revised the DCN circuitry and support the notion that, through electrical coupling with fusiform cells, stellate cells, a class of interneurons in the molecular layer, sense ongoing auditory activity, thus providing a link between AN and PF activity (43, 44). Based on these findings, auditory signals are able to rapidly recruit or suppress stellate cells and control the efficacy of PF activity. Auditory-evoked changes in PF activity through this pathway may provide the trigger for plasticity in presynaptic zinc levels. Moreover, other studies indicate that coincident synaptic activation of PF and AN inputs lead to induction of spike-timing dependent synaptic plasticity (STDP) of parallel fiber inputs (45), by analogy with the climbing fiber and parallel fiber inputs in the cerebellum. According to this scheme, auditory experience-dependent increases in fusiform cell spiking could also provide the trigger to induce plastic changes in PF inputs. Alternatively, because granule cells receive auditory nerve input from higher auditory centers such as auditory cortex, the changes in auditory stimulation might cause changes in vesicular zinc via this pathway (46).

Previous studies have established activity-dependent AMPAR synaptic plasticity via changes in pre- and postsynaptic glutamatergic neurotransmission (47). Such AMPAR plasticity is involved in memory, learning, and development of the CNS and is crucial for the proper functioning and adaptability of the mammalian brain. The sound-dependent plasticity of presynaptic zinc levels and zinc-mediated inhibition of AMPARs (Fig. 4) adds zinc as a key player in the complexity of AMPAR synaptic plasticity in the mammalian brain.

Materials and Methods

All animal procedures were approved by Institutional Animal Care and Use Committees of the University of Pittsburgh. Methods for preparing brain slices, electrophysiological recordings, noise exposure, recording of acoustic brainstem responses, and fluorescence imaging are provided in *SI Materials and Methods*. Data analysis, statistical tests, and detailed values presented in main figures are also provided in *SI Materials and Methods*.

ACKNOWLEDGMENTS. We thank Dr. Elias Aizenman for helpful discussions and critical comments on the manuscript. This work was supported by funding from National Institutes of Health Grants R01-GM065519 (to S.J.L.), F32-DC013734 (to C.T.A.), F32-GM109516 (to J.M.G.), and R01-DC007905 (to T.T.).

1. Traynelis SF, et al. (2010) Glutamate receptor ion channels: Structure, regulation, and function. *Pharmacol Rev* 62(3):405–496.
2. Lerma J, Marques JM (2013) Kainate receptors in health and disease. *Neuron* 80(2):292–311.
3. Zhu S, Paoletti P (2015) Allosteric modulators of NMDA receptors: Multiple sites and mechanisms. *Curr Opin Pharmacol* 20:14–23.
4. Hansen KB, Furukawa H, Traynelis SF (2010) Control of assembly and function of glutamate receptors by the amino-terminal domain. *Mol Pharmacol* 78(4):535–549.
5. Dingledine R, Borges K, Bowie D, Traynelis SF (1999) The glutamate receptor ion channels. *Pharmacol Rev* 51(1):7–61.
6. Bowie D, Mayer ML (1995) Inward rectification of both AMPA and kainate subtype glutamate receptors generated by polyamine-mediated ion channel block. *Neuron* 15(2):453–462.
7. Aizenman CD, Muñoz-Elías G, Cline HT (2002) Visually driven modulation of glutamatergic synaptic transmission is mediated by the regulation of intracellular polyamines. *Neuron* 34(4):623–634.
8. Karakas E, Furukawa H (2014) Crystal structure of a heterotetrameric NMDA receptor ion channel. *Science* 344(6187):992–997.
9. Lee CH, et al. (2014) NMDA receptor structures reveal subunit arrangement and pore architecture. *Nature* 511(7508):191–197.
10. Sobolevsky AI, Rosconi MP, Gouaux E (2009) X-ray structure, symmetry and mechanism of an AMPA-subtype glutamate receptor. *Nature* 462(7274):745–756.
11. O'Neill MJ, Bleakman D, Zimmerman DM, Nisenbaum ES (2004) AMPA receptor potentiators for the treatment of CNS disorders. *Curr Drug Targets CNS Neurol Disord* 3(3):181–194.
12. Vogt K, Mellor J, Tong G, Nicoll R (2000) The actions of synaptically released zinc at hippocampal mossy fiber synapses. *Neuron* 26(1):187–196.
13. Pan E, et al. (2011) Vesicular zinc promotes presynaptic and inhibits postsynaptic long-term potentiation of mossy fiber-CA3 synapse. *Neuron* 71(6):1116–1126.
14. Vergnano AM, et al. (2014) Zinc dynamics and action at excitatory synapses. *Neuron* 82(5):1101–1114.
15. Anderson CT, et al. (2015) Modulation of extrasynaptic NMDA receptors by synaptic and tonic zinc. *Proc Natl Acad Sci USA* 112(20):E2705–E2714.
16. Frederickson CJ, Koh JY, Bush AI (2005) The neurobiology of zinc in health and disease. *Nat Rev Neurosci* 6(6):449–462.
17. Sindreu CB, Varoqui H, Erickson JD, Pérez-Clausell J (2003) Boutons containing vesicular zinc define a subpopulation of synapses with low AMPAR content in rat hippocampus. *Cereb Cortex* 13(8):823–829.
18. Mayer ML, Vyklicky L, Jr, Westbrook GL (1989) Modulation of excitatory amino acid receptors by group IIB metal cations in cultured mouse hippocampal neurones. *J Physiol* 415:329–350.
19. Rassendren FA, Lory P, Pin JP, Nargeot J (1990) Zinc has opposite effects on NMDA and non-NMDA receptors expressed in Xenopus oocytes. *Neuron* 4(5):733–740.
20. Dreixler JC, Leonard JP (1994) Subunit-specific enhancement of glutamate receptor responses by zinc. *Brain Res Mol Brain Res* 22(1-4):144–150.
21. Zhang DQ, Ribelayga C, Mangel SC, McMahon DG (2002) Suppression by zinc of AMPA receptor-mediated synaptic transmission in the retina. *J Neurophysiol* 88(3):1245–1251.
22. Perez-Rosello T, et al. (2013) Synaptic Zn2+ inhibits neurotransmitter release by promoting endocannabinoid synthesis. *J Neurosci* 33(22):9259–9272.
23. Oertel D, Young ED (2004) What's a cerebellar circuit doing in the auditory system? *Trends Neurosci* 27(2):104–110.
24. Frederickson CJ, Howell GA, Haigh MD, Danscher G (1988) Zinc-containing fiber systems in the cochlear nuclei of the rat and mouse. *Hear Res* 36(2-3):203–211.
25. Faber DS, Korn H (1991) Applicability of the coefficient of variation method for analyzing synaptic plasticity. *Biophys J* 60(5):1288–1294.
26. Tsien RW, Malinow R (1991) Changes in presynaptic function during long-term potentiation. *Ann N Y Acad Sci* 635:208–220.
27. Paoletti P, Vergnano AM, Barbour B, Casado M (2009) Zinc at glutamatergic synapses. *Neuroscience* 158(1):126–136.
28. Cole TB, Wenzel HJ, Kafer KE, Schwartzkroin PA, Palmiter RD (1999) Elimination of zinc from synaptic vesicles in the intact mouse brain by disruption of the ZnT3 gene. *Proc Natl Acad Sci USA* 96(4):1716–1721.
29. Perez-Rosello T, Anderson CT, Ling C, Lippard SJ, Tzounopoulos T (2015) Tonic zinc inhibits spontaneous firing in dorsal cochlear nucleus principal neurons by enhancing glycinergic neurotransmission. *Neurobiol Dis* 81:14–19, 1.
30. Hansen KB, Ogden KK, Yuan H, Traynelis SF (2014) Distinct functional and pharmacological properties of Triheteromeric GluN1/GluN2A/GluN2B NMDA receptors. *Neuron* 81(5):1084–1096.
31. Miller PS, Da Silva HM, Smart TG (2005) Molecular basis for zinc potentiation at strychnine-sensitive glycine receptors. *J Biol Chem* 280(45):37877–37884.
32. Rubio ME, Juiz JM (1998) Chemical anatomy of excitatory endings in the dorsal cochlear nucleus of the rat: Differential synaptic distribution of aspartate aminotransferase, glutamate, and vesicular zinc. *J Comp Neurol* 399(3):341–358.
33. Petralia RS, Rubio ME, Wang YX, Wenthold RJ (2000) Differential distribution of glutamate receptors in the cochlear nuclei. *Hear Res* 147(1-2):59–69.
34. Zastrow ML, et al. (2015) Reaction-based probes for imaging mobile zinc in live cells and tissues [published online ahead of print September 23, 2015]. *ACS Sensors*, 10.1021/acssensors.5b00022.
35. Wenthold RJ, Petralia RS, Blahos J II, Niedzielski AS (1996) Evidence for multiple AMPA receptor complexes in hippocampal CA1/CA2 neurons. *J Neurosci* 16(6):1982–1989.
36. Nakashima AS, Dyck RH (2009) Zinc and cortical plasticity. *Brain Res Brain Res Rev* 59(2):347–373.
37. Kujawa SG, Liberman MC (2009) Adding insult to injury: Cochlear nerve degeneration after "temporary" noise-induced hearing loss. *J Neurosci* 29(45):14077–14085.
38. Li S, Kalappa BI, Tzounopoulos T (2015) Noise-induced plasticity of KCNQ2/3 and HCN channels underlies vulnerability and resilience to tinnitus. *eLife* 4, 10.7554/eLife.07242.
39. Salazar G, et al. (2004) The zinc transporter ZnT3 interacts with AP-3 and it is preferentially targeted to a distinct synaptic vesicle subpopulation. *Mol Biol Cell* 15(2):575–587.
40. Lavoie N, et al. (2011) Vesicular zinc regulates the Ca2+ sensitivity of a subpopulation of presynaptic vesicles at hippocampal mossy fiber terminals. *J Neurosci* 31(50):18251–18265.
41. Jia Y, Jeng JM, Sensi SL, Weiss JH (2002) Zn2+ currents are mediated by calcium-permeable AMPA/kainate channels in cultured murine hippocampal neurones. *J Physiol* 543(Pt 1):35–48.
42. Armstrong N, Gouaux E (2000) Mechanisms for activation and antagonism of an AMPA-sensitive glutamate receptor: Crystal structures of the GluR2 ligand binding core. *Neuron* 28(1):165–181.
43. Apostolides PF, Trussell LO (2013) Regulation of interneuron excitability by gap junction coupling with principal cells. *Nat Neurosci* 16(12):1764–1772.
44. Apostolides PF, Trussell LO (2014) Superficial stellate cells of the dorsal cochlear nucleus. *Front Neural Circuits* 8:63.
45. Zhao Y, Rubio M, Tzounopoulos T (2011) Mechanisms underlying input-specific expression of endocannabinoid-mediated synaptic plasticity in the dorsal cochlear nucleus. *Hear Res* 279(1-2):67–73.
46. Ryugo DK, Haenggeli CA, Doucet JR (2003) Multimodal inputs to the granule cell domain of the cochlear nucleus. *Exp Brain Res* 153(4):477–485.
47. Malenka RC, Bear MF (2004) LTP and LTD: An embarrassment of riches. *Neuron* 44(1):5–21.
48. Tzounopoulos T, Kim Y, Oertel D, Trussell LO (2004) Cell-specific, spike timing-dependent plasticities in the dorsal cochlear nucleus. *Nat Neurosci* 7(7):719–725.
49. Balakrishnan V, Trussell LO (2008) Synaptic inputs to granule cells of the dorsal cochlear nucleus. *J Neurophysiol* 99(1):208–219.
50. Fujino K, Oertel D (2003) Bidirectional synaptic plasticity in the cerebellum-like mammalian dorsal cochlear nucleus. *Proc Natl Acad Sci USA* 100(1):265–270.
51. Woodroofe CC, Masalha R, Barnes KR, Frederickson CJ, Lippard SJ (2004) Membrane-permeable and -impermeable sensors of the Zinpyr family and their application to imaging of hippocampal zinc in vivo. *Chem Biol* 11(12):1659–1666.